HADRONIC FINAL STATES IN DIFFRACTION AT HERA [a]

A. BUNYATYAN
Max-Planck-Institut für Kernphysik,
Saupfercheckweg 1, 69117 Heidelberg, Germany
and Yerevan Physics Institute, Armenia
E-mail: bunar@mail.desy.de

Representing the H1 and ZEUS Collaborations

Measurements are presented of global event shapes, energy flow, charged particle multiplicity, high p_T jets and open charm production in diffractive ep scattering, performed by the H1 and ZEUS Collaborations at HERA. The results are in agreement with models based on the parton densities extracted from inclusive ep diffractive scattering at HERA and support the hypothesis that the momentum of the diffractive exchange is carried largely by hard gluons.

1 Introduction

There are considerable attempts to understand the underlying dynamics of diffractive interactions in terms of quantum chromodynamics. At HERA, the contribution to the proton structure function from diffractive processes has been measured, for example, in terms of a diffractive structure function $F_2^{D(3)}$ [1,2]. Within the DGLAP ansatz, diffractive parton distributions have been extracted that are dominated at low Q^2 by gluons carrying large fractions of the exchanged momentum. With the assumption of diffractive factorization, i.e. a flux of colourless objects and partonic coupling, the parton distributions for the Pomeron extracted from $F_2^{D(3)}$ are expected to universally describe hard diffractive interactions once perturbation theory may be applied.

The analysis of hadronic final states in diffractive interactions provides an independent test of this picture. In this report some recent results of the H1 and ZEUS experiments are reviewed.

2 Selection of diffractive events

The generic diffractive process $ep \to eXY$ is illustrated in Fig.1. The systems X and Y are defined by the largest gap in rapidity of final state hadrons and Y is the system closest to the outgoing proton direction. The diffractive process can be described in terms of:

$$M_X^2 = p_X^2 \qquad M_Y^2 = p_Y^2 \qquad t = (p_p - p_Y)^2 \qquad x_{I\!P} = \frac{q \cdot (p_p - p_Y)}{q \cdot p_p}.$$

[a] Talk given at the International Conference (VIIIth'Blois Workshop) on Elastic and Diffractive Scattering, EDS99, June 28–July 2, 1999, Protvino, Russia

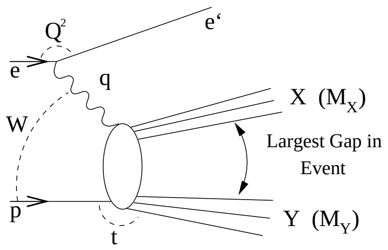

$$s = (p_e + p_p)^2 \quad Q^2 = -q^2$$

$$W^2 = (q + p_p)^2$$

$$x = \frac{Q^2}{2q \cdot p_p} \qquad y = \frac{q \cdot p_p}{p_e \cdot p_p}$$

Figure 1: Illustration of the generic diffractive process $ep \to eXY$

t is the squared four-momentum transferred between the photon and the incoming proton, and $x_{I\!P}$ is the fraction of the proton beam momentum transferred to the diffractive system X. Experimentally, in analyses of hadronic final states at HERA, two different methods are used to select diffractive dissociation:

• Detection of the leading proton (LPS method): both experiments have dedicated proton spectrometers to detect and measure directly protons which are produced at very small scattering angles ($\theta \lesssim 1\ mrad$). The data sample selected with this method corresponds to single photon dissociation ($M_Y \equiv M_p$).

• Large Rapidity Gap selection (LRG method): diffractive events are characterized by a rapidity gap between the two hadronic subsystems X and Y of the size $\Delta\eta \simeq ln(W^2/M_X^2)$. The gap is identified by an absence of activity in the forward part of detector. Since the system Y is not detected, the selected data sample also contains events where the proton dissociates to low mass states (e.g. $M_Y \lesssim 1.6\ GeV$ in H1 analyses).

3 Models for diffractive hard scattering

The models for diffractive hard scattering which are used in analyses for comparison with data can be in general subdivided into three classes:

• Factorizible models (e.g. Monte–Carlo programs RAPGAP[3] and POMPYT[4]): In these models the photon–proton diffractive scattering is factorized as a flux of spacelike Pomerons from the proton and subsequent photon–Pomeron interaction. The parton densities in the Pomeron have been analyzed in the form of QCD fits to $F_2^{D(3)}$ data [1,15]. The expected topology of the hadronic final state depends strongly on the partonic structure of the Pomeron. For a quark dominated Pomeron the final state in lowest order is defined by a $q\bar{q}$ configuration with low transverse momentum relative to the photon direction in the $\gamma^* I\!P$ center of mass (CM) frame. A gluon dominated Pomeron interacts largely by the boson–gluon fusion (BGF) mechanism with a $q\bar{q}g$ system in the final state: the transverse momenta of the outgoing partons and the amount of gluon radiation are therefore expected to be larger than in the case of a quark dominated Pomeron.

• Two-Gluon models (e.g. Monte–Carlo program RIDI [5]):
These models describe the diffractive $\gamma^* p$ interaction in terms of the elastic scattering of partonic fluctuations of the photon ($q\bar{q}$, $q\bar{q}g$,...) from the proton via the exchange of two gluons in a net colour–singlet configuration. The simplest $q\bar{q}$ state is relevant only at small transverse momenta $\hat{p}_T$ of the outgoing partons due to colour transparency effect. At large $\hat{p}_T$ the cross–section is therefore dominated by the scattering of $q\bar{q}g$ and higher multiplicity components.

• Soft Colour Interactions (SCI) (e.g. Monte–Carlo program LEPTO [6]):
In this model LRG events are the result of normal ep DIS scattering with subsequent soft interactions between the outgoing partons. These interactions alter the final–state colour configurations, and hence may give rise to large rapidity gaps.

4 Global Event Shapes

The topological features of the hadronic final state in γ^* dissociation were studied at HERA by analyzing the event–shape variables thrust $\langle T \rangle$ and sphericity $\langle S \rangle$ [7,8]. These variables have been used extensively in e^+e^- experiments at various CM energies [9], and thus are interesting for a comparison with diffractive DIS data. Figures 2a,b show the average values of thrust and sphericity as a function of M_X for ZEUS DIS events, selected with the leading proton (LPS) method. For comparison, the data from e^+e^- annihilation events are plotted at $M_X = \sqrt{s_{e^+e^-}}$. The following features are observed:

• $\langle T \rangle$ increases ($\langle S \rangle$ decreases) with M_X. This signifies an increasing back-to-back correlation of the momentum flow as the final state mass increases, and the thrust direction defines the topological axis of the event.

• There is a striking similarity between the energy dependence of $\langle T \rangle$ and $\langle S \rangle$ in e^+e^- annihilation and in virtual photon dissociation, both in shape and absolute values. This observation suggests that the diffractive DIS hadronic system can be predominantly viewed as a simple $q\bar{q}$ system. On the other hand, the RAPGAP Monte–Carlo, which implements a gluon dominated Pomeron and uses the ARIADNE fragmentation scheme can reproduce the event shape variables well. The RIDI Monte–Carlo fails to describe ZEUS data, a deficiency that might be remedied by tuning the relative contributions of $q\bar{q}$ and $q\bar{q}g$ processes.

Also plotted in Fig.2a are the average thrust values measured by H1 where the diffractive DIS sample is tagged with large rapidity gaps (LRG). The $\langle T \rangle$ of H1 LRG events is systematically lower than in the ZEUS LPS data and e^+e^- annihilation events at low M_X. This result $\langle T \rangle_{H1} < \langle T \rangle_{e^+e^-}$ means that the parton multiplicities higher than a simple $q\bar{q}$ state are more important in H1 LRG DIS events than in e^+e^- annihilation. The discrepancy between the H1 and ZEUS results is still under investigation, but it may be due to different methods of diffractive event tagging.

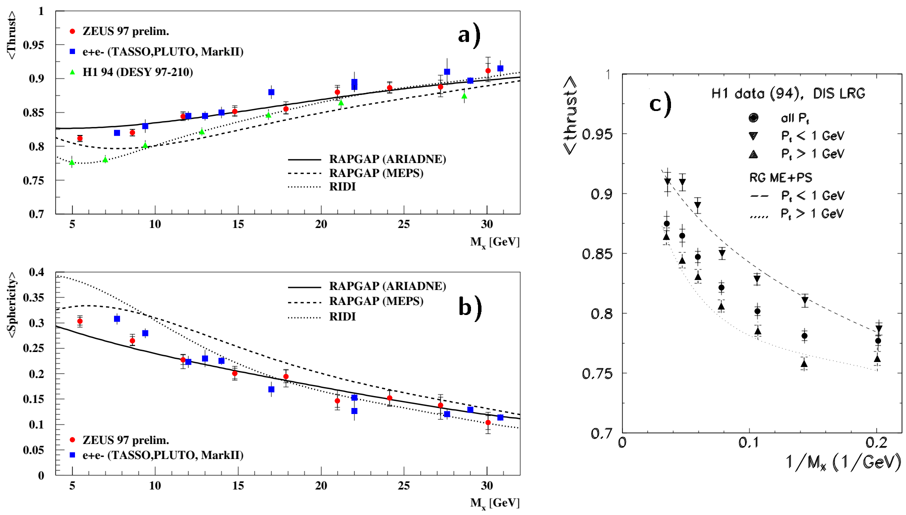

Figure 2: Average thrust and sphericity distributions for ZEUS and H1 diffractive DIS data as a function of M_X $(1/M_X)$, and for e^+e^- annihilation data as a function of $\sqrt{s_{ee}}$. The ZEUS data correspond to kinematical range: $4 < Q^2 < 90\ GeV^2$, $4 < M_X < 35\ GeV$, $0.0003 < x_{I\!P} < 0.03$, $52 < W < 250\ GeV$, and the H1 data- to the range: $10 < Q^2 < 100\ GeV^2$, $4 < M_X < 36\ GeV$, $y < 0.5\ GeV$, $x_{I\!P} < 0.05$, $|t| < 1\ GeV^2$, $M_Y < 1.6\ GeV$.

Given the thrust axis, two thrust jets can be defined as groups of particles with positive or negative momentum components along the thrust axis. In Fig.2c the average thrust is shown as a function of $1/M_X$ for events with differing transverse thrust jet momentum relative to the proton beam direction. At each M_X point the average thrust for large P_t is lower than for small P_t, indicating the presence of configurations with at least 3 non-collinear partons. RAPGAP predictions for a mixture of $q\bar{q}$ and $q\bar{q}g$ configurations confirm this conclusion.

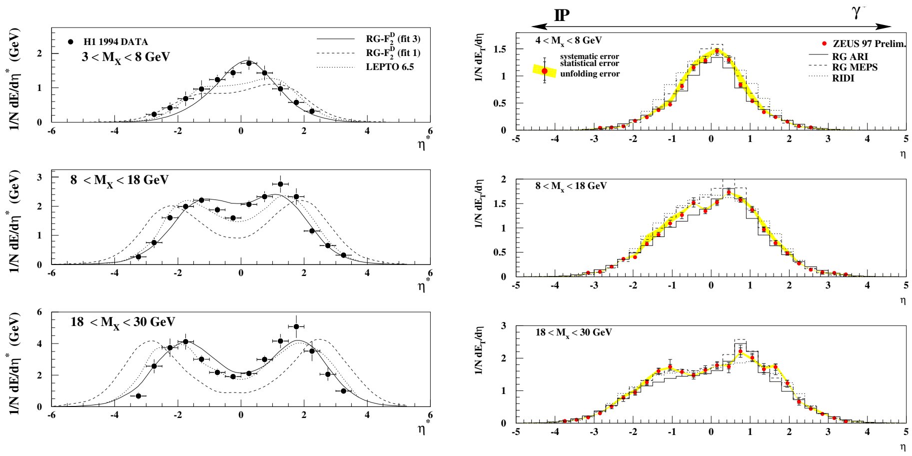

Figure 3: The energy flow from H1 **(a)** and the transverse energy flow from ZEUS **(b)** for the diffractive DIS data as a function of pseudorapidity for 3 different M_X intervals.

5 Hadron Production

Figure 3 (left) shows the event-normalized energy flow against pseudorapidity $\eta^* = -\ln(\tan\ \theta/2)$ in three regions of M_X, where θ is the polar angle of energy deposit with respect to the a $\gamma^* I\!P$ CM axis. The distribution is approximately symmetrical about $\eta^* = 0$, with similar levels of energy flow in the two hemispheres. At higher masses, $M_X > 8\ GeV$, a two–peaked structure is seen, indicating that the major topological property of these events is of a 2-jet nature (current jet and remnant jet). The data are well described by the RAPGAP model with the gluon dominated Pomeron parton densities ($RG - F_2^D$-fit 3), and for $M_X > 8\ GeV$ by LEPTO, whereas the the RAPGAP model with the quark dominated Pomeron parton densities ($RG - F_2^D$-fit 1) model predicts too much energy flow at the largest accessible pseudorapidity and fails to account for the observed energy flow in the central region. A similar behavior has been seen by the ZEUS experiment using the LPS selection method [8]. Figure 3 (right) shows the distribution of transverse energy as a function of η^* measured by ZEUS. A slight asymmetry is visible at high M_X with less energy going in the Pomeron direction, which indicates a suppression of particle production associated with the Pomeron remnant. This asymmetry is predicted from the Monte–Carlo.

The observed features can be related to the gluon content of the Pomeron and to the role of BGF. The transverse momentum generated by this process reduces the accessible pseudorapidity range along the $\gamma^* I\!P$ axis at fixed M_X and induces additional energy flow in more central regions.

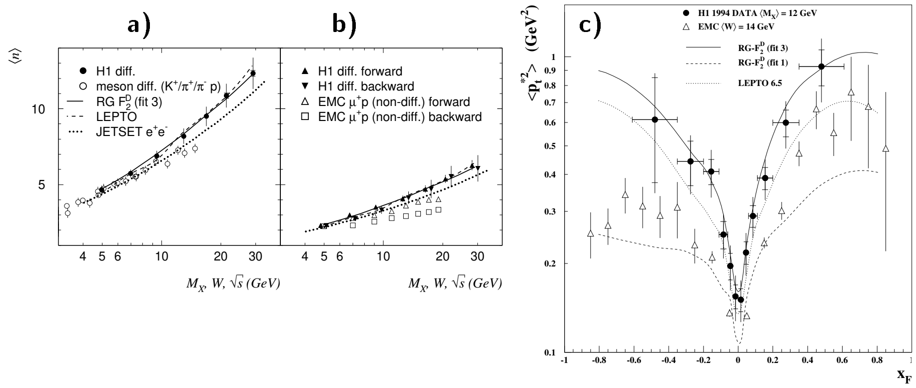

Figure 4: Average charged particle multiplicity in full phase space **(a)** and in single hemispheres **(b)** as a function of M_X. Seagull plot **(c)** showing H1 diffractive DIS data together with EMC μp DIS data.

Complementary to the energy flow analyses we studied the multiplicity of charged particles [11]. Figure 4a shows the dependence of the mean charged particle multiplicity $\langle n \rangle$ on M_X for the H1 diffractive DIS data compared with results from meson diffraction [12] and e^+e^- annihilation (modeled by JETSET). The multiplicities for all these processes are similar at low masses, but for $M_X \gtrsim 10\ GeV$ the multiplicity grows faster with mass in diffractive DIS than in other processes. It may be concluded from this result that low-mass diffraction in hadron collisions and photon dissociation in DIS at HERA can be interpreted as the hadronization of a single string. High-mass diffraction involves additional mechanisms besides $q\bar{q}$ fragmentation and gluon bremsstrahlung from the quark. Figure 4b shows the mean multiplicity in the forward and backward hemispheres separately. There is no evidence for an asymmetry between the two hemispheres, in contrast to what is observed in fixed-target μp DIS.

Confirmation of the general trends discussed above is obtained from the "seagull plot" distribution, which was studied both by H1 [10] and ZEUS [8]. The H1 result is shown in Fig.4c, in which the mean transverse momentum squared, $\langle p_T^{*2} \rangle$, is plotted as a function of the Feynman-x variable, $x_F = 2p^*_{||}/M_X$, where $p^*_{||}$ is the component of the particle's momentum in the direction of the incoming proton. The plot shows a greater degree of symmetry than is present in the EMC $\gamma^* p$ data [13]. This is consistent with having a more point-like partonic system in the target fragmentation hemisphere in the diffractive data than in $\gamma^* p$ data, where the extended nature of the proton remnant leads to a restricted phase space for parton radiation. $\langle p_T^{*2}\rangle$ is significantly higher in the H1 diffractive data than in $\gamma^* p$ data which can be attributed to the transverse momentum generated by the BGF process. This behavior is well described by the gluon dominated Pomeron model (RAPGAP-fit 3) whereas the $\langle p_T^{*2}\rangle$ values predicted by the quark dominated Pomeron model (RAPGAP-fit 1) model are too low at all x_F.

In conclusion, the studies of global event shapes, energy flow and charged particle multiplicity support the conclusion reached in the analysis of the diffractive structure function $F_2^{D(3)}$ that, at low Q^2, the momentum of the diffractive exchange is carried largely by hard gluons.

6 High p_T Jet production

Jet production has been investigated both in photoproduction ($Q^2 \sim 0$) and DIS ($Q^2 \gg 0$) [14,15]. Events were selected which contained two jets with transverse energies above 5 GeV (H1) and 6 GeV (ZEUS). Figure 5a shows the photoproduction cross-section differential in the jet energy E_T^{jet} transverse to the $\gamma^* I\!P$ interaction axis. The result is compared to the model predictions, which are based on the combined QCD analysis of the diffractive structure function in DIS and of the di-jet cross-sections in photoproduction, and which require a substantial hard momentum component of gluons in the Pomeron [15]. The models describe the data distributions well (also in other variables), confirming the results of other HERA diffractive analyses that a large gluon component is required in the Pomeron parton distributions.

The jet cross–section was measured also differentially in the variables x_γ and $z_{I\!P}$ which can be interpreted as a fraction of photon and Pomeron momenta respectively carried by the partons involved in the hard interactions. The cross-section $d\sigma/dx_\gamma^{obs}$ is shown in Fig.5b. The distribution peaks at high values of x_γ, with a pronounced tail that extends to low x_γ values. This result shows the presence of both a direct ($x_\gamma = 1$) and a resolved ($x_\gamma < 1$) component in diffractive di-jet photoproduction and is in good agreement with Monte–Carlo expectations.

The cross-section $d\sigma/dz_{I\!P}^{jet}$ in H1 photoproduction data is shown in Fig.6a. It indicates the sizeable contribution to di-jet production from events in which a large fraction of the Pomeron momentum participates in the hard scattering.

The model in which the diffractive parton distributions consist solely of quarks at the starting scale underestimates the cross-section by factor 5 (not shown in plots). The POMPYT Monte–Carlo with hard gluon simulation

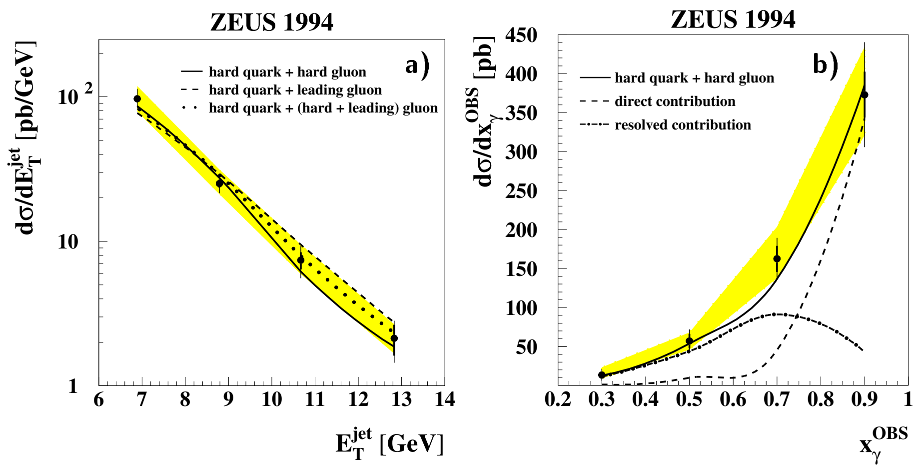

Figure 5: Differential cross-section for photoproduction of di-jets: **(a)** as function of E_T^{jet} and **(b)** as function of x_γ^{obs} (ZEUS). The shaded band displays the uncertainty due to the absolute energy scale of the jets.

reproduces the shape of distribution but lies slightly above the data. The difference in normalization between the data and Monte–Carlo predictions can be explained by following argument. In resolved photon interactions multiple interactions between spectator partons might destroy rapidity gaps, an effect which would represent a breaking of diffractive factorization. This effect is not expected to be present in direct photon interactions. Since no full calculations of spectator interactions in diffractive photoproduction exist, we compare the data to the POMPYT models after applying constant weighting factors, so called "survival probabilities", $< S >= 0.4 \div 0.6$ to all events generated with $x_\gamma < 0.8$. The introduction of this factor improves the distributions at all $z_{I\!P}^{jet}$. At the Tevatron, the comparison of diffractive di-jet production data with models suggest that the rapidity gap survival probability may be as small as 0.1 for $p\bar{p}$ interactions at $\sqrt{s} = 1800\ GeV$ [17]. Within the context of this very crude model, a possible interpretation is therefore that the rapidity gap survival probability for resolved photoproduction at HERA is larger that for $p\bar{p}$ interactions at higher energies at Tevatron.

The DIS di-jet production cross-section differential in $z_{I\!P}^{jets}$ is presented and compared to Monte–Carlo prediction in Fig.6b. There is a significant contribution at the largest $z_{I\!P}^{jets}$ and the differential cross-section increases as $z_{I\!P}^{jets}$ decreases. The calculation for the $q\bar{q}$ Fock state [16] is compared via RAPGAP simulation. This model falls short of the data. Higher parton multiplicities are

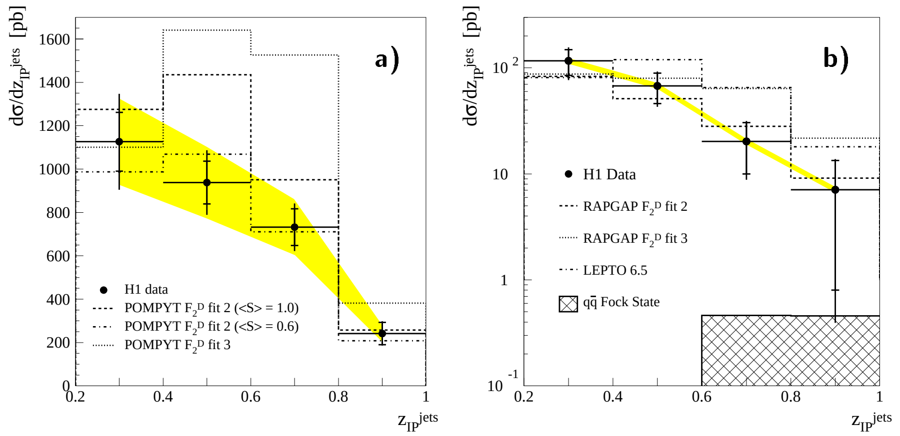

Figure 6: Differential cross-section as a function of $z_{I\!P}^{jet}$ in **(a)** photoproduction and **(b)** DIS regimes. The shaded band shows the overall normalization uncertainties.

presumably dominant in the kinematic regime studied here.

7 Open charm production

Open charm production in diffractive DIS is a sensitive probe of the underlying partonic nature of the production mechanism. Both the H1 and ZEUS Collaborations have observed a signal of $D^{*\pm}(2010)$ mesons in diffractive DIS interactions [18,19]. The D^* mesons are reconstructed using the decay channels

$$\begin{aligned} D^{*\pm} &\to D^0\pi^{\pm} \to (K\pi)\pi^{\pm} \\ &\qquad\qquad\;\; \to (K\pi\pi\pi)\pi^{\pm} \end{aligned}$$

H1 uses only the $K\pi\pi$ mode whereas ZEUS uses both.

The fraction of diffractively produced D^* to all D^* produced in a given kinematic region was measured by ZEUS. Within the errors the result is rather independent of Q^2 and W and is equal to $7.0 \pm 1.3^{+1.7}_{-1.8}$ % ($D^* \to K\pi\pi$), $8.9 \pm 2.4^{+1.7}_{-1.6}$ % ($D^* \to K4\pi$). These numbers are consistent with the fraction of the total ep cross-section attributed to diffractive scattering [2].

The differential D^* cross-sections measured by ZEUS in $D^* \to K4\pi$ decay channel are shown in Fig.7. Results are compared with different model predictions [5,20,21]. Given the large statistical errors, all distributions are reasonably well reproduced by the different predictions. However, it was found that the data favour predictions made with a gluon–dominated compared to a quark–dominated Pomeron in the resolved Pomeron model, and favour predictions of a two–gluon model which includes higher order corrections. Similar measurements were done by ZEUS using the $D^* \to K\pi\pi$ channel. Good agreement between the two decay channels was obtained.

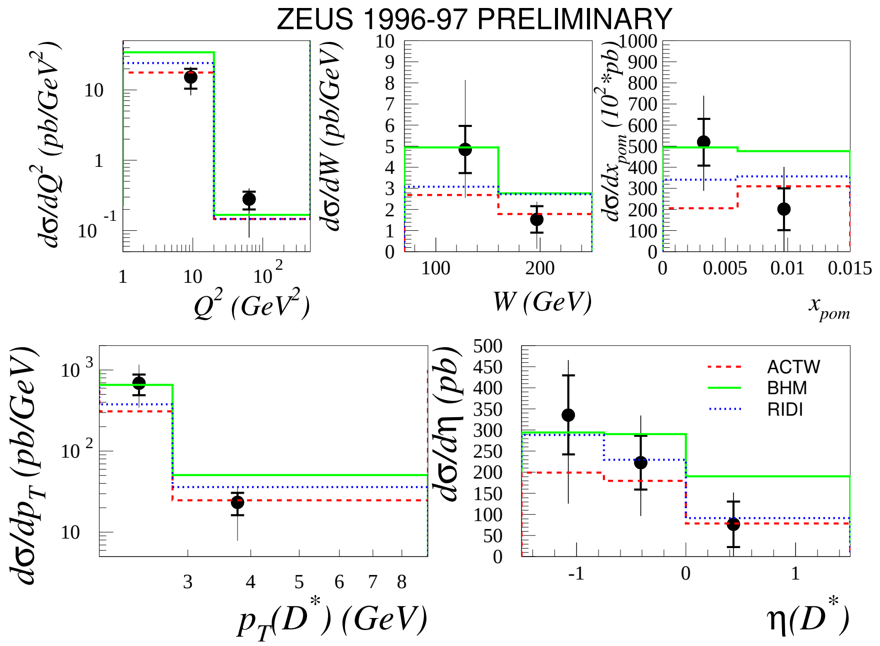

Figure 7: The differential diffractive D^* cross-sections as a function of Q^2, W, $x_{I\!P}$, $p_T^*(D^*)$, $\eta(D^*)$ (ZEUS).

The differential cross-sections measured by H1 are shown in Fig.8 as functions of p_T^* and the hadronic observable $z_{I\!P}^{obs}$, defined by the equation:

$$z_{I\!P} = \beta \cdot (1 + \frac{\hat{s}}{Q^2}) \approx \frac{(M_{c\bar{c}}^2 + Q^2)}{(M_X^2 + Q^2)} = z_{I\!P}^{obs}$$

The resolved Pomeron approach reproduces well the shape of the spectra and in particular the fact that the data show a sizeable fraction of charm production in the low $z_{I\!P}$ region. However, while the model agrees with the ZEUS data, it falls

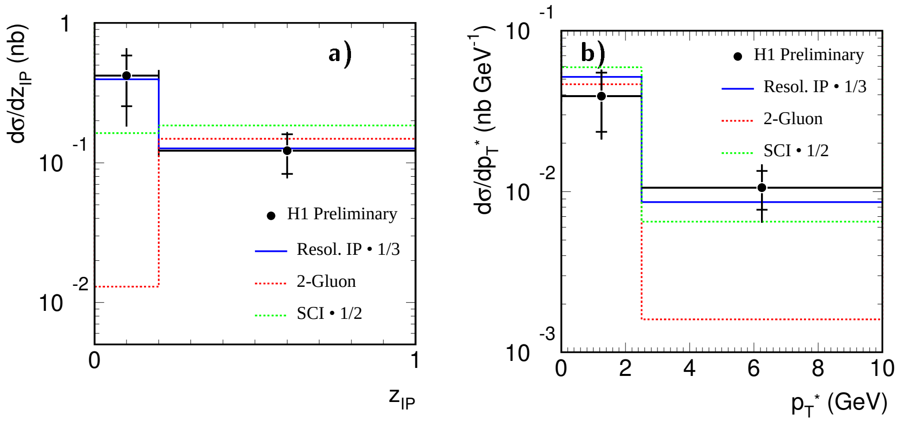

Figure 8: The differential diffractive D^* cross-sections as a function of $z_{I\!P}$ and p_T^* (H1).

a factor of 2 to 3 below the H1 data. Reasons for this discrepancy are still under investigation. The two gluon model for exclusive charm production $\gamma^* + p \to c\bar{c} + p$, in contrast to the resolved Pomeron model, does not describe the region of low $z_{I\!P}$ and high p_T^*. It is apparent that the higher order contributions such as $\gamma^* + p \to c\bar{c}g + p$ are needed.

8 Summary

Some properties of hadronic final states in diffractive ep interactions at HERA have been presented.

Measurements of event shape evolution with M_X, the energy flow, charged particle multiplicities are in general consistently described by resolved Pomeron models with gluon dominated parton densities evolving with DGLAP. These studies confirm the results of the inclusive $F_2^{D(3)}$ measurements, however there are some puzzles to be understood in the rate of di-jet events and D^* production.

References

1. H1 Collab., *Z. Phys.* C **76**, 613 (1997)
2. ZEUS Collab., *Z. Phys.* C **68**, 569 (1995);
   ZEUS Collab., *Eur. Phys. J* C **6**, 43 (1999)
3. H.Jung, *Comp. Phys. Comm.* **86** (1995) 147

4. P.Bruni, G.Ingelman, Proc. of the Europhysics Conference, Marseilles, July 1993, 595
5. M.G.Ryskin, Sov. Journ. Nucl. Phys. **52** (1990) 529;
M.G.Ryskin and A.Solano, Proc. of Workshop *'Monte–Carlo Generators for HERA Physics',* Ed. G.Grindhammer, G.Ingelman, H.Jung and T.Doyle (1999), Hamburg, Germany
6. G.Ingelman, A.Edin, J.Rathsman, *Comp. Phys. Comm.* **101** (1997) 108
7. H1 Collab., *Eur. Phys. J* C **1**, 495 (1998)
8. ZEUS Collab., Contributed paper N505 to Intern. Europhys. Conference HEP99, Tampere, Finland, Jul.1999
9. PLUTO Collab., *Z. Phys.* C **12**, 297 (1982);
MARK II Collab., *Phys. Rev.* D **37**, 1 (1988);
TASSO Collab., *Z. Phys.* C **47**, 187 (1990);
AMY Collab., *Phys. Rev.* D **41**, 2675 (1990);
DELPHI Collab., *Z. Phys.* C **73**, 229 (1997)
10. H1 Collab., *Phys. Lett.* B **428**, 206 (1998)
11. H1 Collab., *Eur. Phys. J* C **5**, 439 (1998)
12. NA22 Collab., *Z. Phys.* C **55**, 531 (1992);
F.C.Winkelman et al.,*Phys. Rev. Lett.* **32**, 121 (1974);
R.L.Cool et al.,*Phys. Rev. Lett.* **48**, 1451 (1982)
13. EMC Collab., *Phys. Lett.* B **149**, 415 (1984);
EMC Collab., *Z. Phys.* C **35**, 417 (1987)
14. H1 Collab., *Eur. Phys. J* C **6**, 421 (1999)
15. H1 Collab., *Eur. Phys. J* C **5**, 41 (1998)
16. J.Bartels, H.Lotter, M.Wüsthoff, *Phys. Lett.* B **379**, 239 (1996);
J.Bartels et al., *Phys. Lett.* B **386**, 389 (1996)
17. CDF Collab., *Phys. Rev. Lett.* **79**, 2636 (1997);
K. Borras (CDF), P.Rubinov (D0), In Proc. of the 6th Intern. Workshop on DIS and QCD, Brussels, Belgium, April 1998, pp. 422-429
18. ZEUS Collab., Contributed paper N527 to Intern. Europhys. Conference HEP99, Tampere, Finland, Jul.1999
19. H1 Collab., Contributed paper N157ag to Intern. Europhys. Conference HEP99, Tampere, Finland, Jul.1999
20. L.Alvero et al., *Phys. Rev.* D **59**, 74022 (1999)
21. W.Buchmüller, A.Hebecker and M.F.McDermott, *Phys. Lett.* B **404**, 353 (1997)